Bull. Min. Res. Exp. (2018) 157: 153-164

Bulletin of the Mineral Research and Exploration

http://bulletin.mta.gov.tr

Geochemical characteristics of Gabbroic rocks in Zyarat in North East of Iran

Ghassem AZIZZADEH[a], Mostafa RAGHIMI[b], Seyed Jamal SHEIKHZAKARIAEE[c*] and Aziz RAHIMI CHAKDEL[d]

[a]*Department of Geology, Science and Research Branch, Islamic Azad University, Tehran*
[b]*Department of Geology, Science and Research Branch, Islamic Azad University, Tehran*
[c]*Department of Geology, Science and Research Branch, Islamic Azad University, Tehran*
[d]*Department of Geology, Science and Research Branch, Islamic Azad University, Tehran.*

Research Article

Keywords:
Gabbro, alkaline, geochemistry, Zyarat, OIB.

ABSTRACT

The mafic rocks outcrops exposed in the South of Gorgan, northeastern of Iran. These gabbroic rocks are intruded into the Middle–Upper Paleozoic sedimentary rocks and Gorgan schist units representing a part of the north Gondwana province. Petrography studies of these rocks show medium to coarse grained sizes and the texture varies from ophitic to intergranular under polarized microscope. The mineralogical composition of mafic dykes is dominated by large crystals of clinopyroxene + orthopyroxene + plagioclase and hornblende. These rocks can be classified as gabbroic rock. Geochemical studies show that these rocks have low to medium K_2O contents. The trace element data shows low La/Nb ratios and LREE enrichment (La/Yb 10–21.4). The high LREE/HREE ratios and low Y content corresponding high Ti/Y ratios of the gabbros suggest that they could be derived from melt fractions of a garnet stable source. Considering that the REE plot and tectonic diagrams of the region's gabbro are similar to that of OIB (Ocean island basalt), the former's origin is the same as that of OIB magmas.

Received Date: 13.03.2017
Accepted Date: 21.12.2017

1. Introduction

Based on geological divisions, the studied area is located in the eastern Alborz zone (Gansser, 1951) (Figure 1), which was the northern margin of the Gondwana during Palaeozoic (Stöcklin, 1974; Salehi Rad, 1979; Berberian and King, 1981; Davoudzadeh et al., 1986; Davoudzadeh and Weber-Diefenbach, 1987; Şengör, 1990; Alavi, 1991, 1996; Stampfli and Borel, 2002; Allen et al., 2003; Horton et al., 2008; Sinha, 2012, 2013).

Mid Paleozoic mafic intrusions, sills, dykes, volcanic tuffs and lava flows are widespread in Iran (Jenny, 1977*a*; Delaloye et al., 1981; Alavi, 1996; Wendt et al., 2005). The most prominent volcanic activity is expressed by up to 600 m– thick andesitic lavas and tuffs in the Soltan Maidan Formation in the eastern Alborz, which are ascribed to the breakup of the northern margin of Gondwana (Jenny, 1977*b*; Alavi, 1996). The Soltan Maidan volcanics are unconformably overlain by conglomerate and sandstones of Lower Devonian age (Wendt et al., 2005). However, in some places Lower to Middle Ordovician age deposits (Lashkarak Formation) underlie these volcanic rocks. Thus, the Soltan Maidan volcanic rocks are generally considered as Silurian in age (e.g., Sharabi, 1990; Zamani Pedram and Hossieni, 2003; Rahimi Chakdel, 2007; Raghimi, 2010).

Due to the difficult condition of studies and loss of outcrop, there is no detailed petrographic study on gabbroic rocks so the purpose of the present research is to carry out a petrological evaluation of these rocks by petrographic and geochemical studies. Petrogenetic studies can provide important information for understanding the mantle source of the magmas and

* *Corresponding author: Seyed Jamal SHEIKHZAKARIAEE, j.sheikhzakaria@gmail.com*
htpp://dx.doi.org/ 10.19111/bulletinofmre.413716

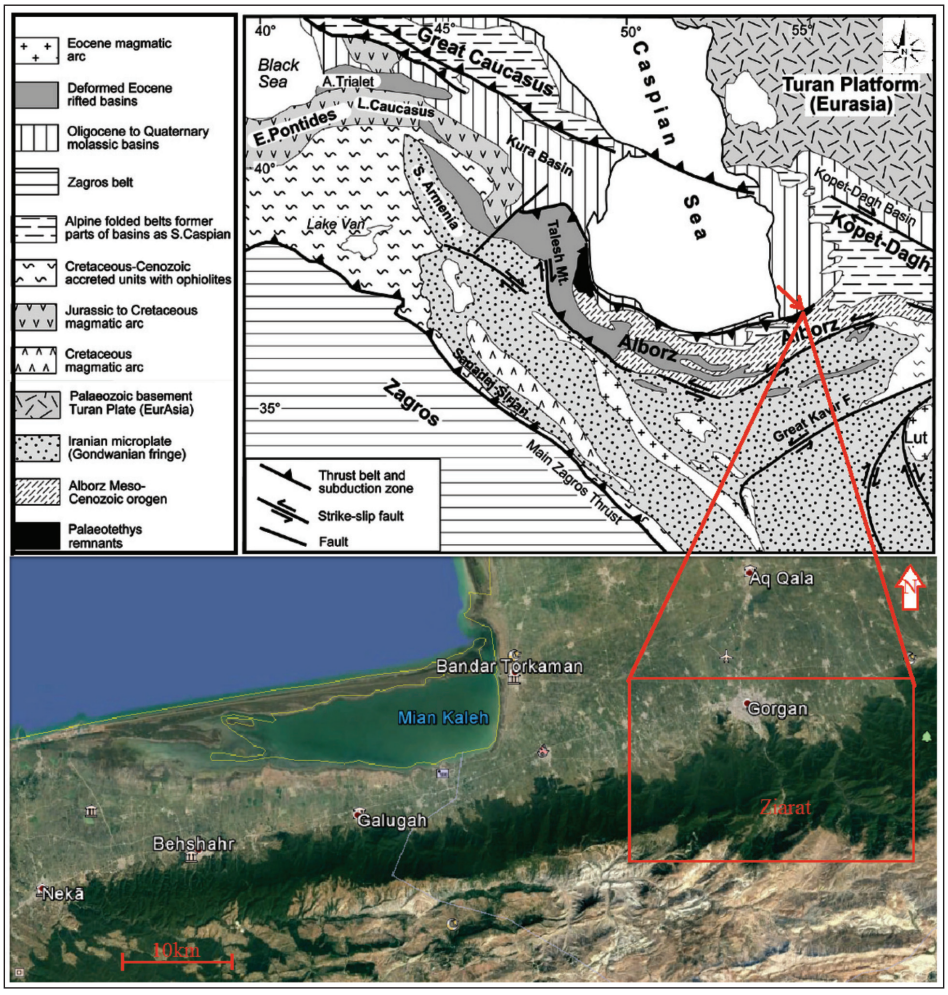

Figure 1- General tectonic map of North Iran and of the South Caspian region (modified from Brunet et al., 2003).

the tectonic evolution of the orogenic belt and adjacent regions (Gorring and Kay, 2001).

2. Geographical Location

The study area is situated approximately 5 km south of the Gorgan city, in northeastern Iran. In this area, Paleozoic rock units comprise Upper Ordovician, Silurian and Upper Carboniferous deposits. The metamorphic rocks (Gorgan schists), as one of the important geological units in Iran, are formed mainly of low-metamorphic rocks such as slate, phyllite, chlorite schist, greenschist and micaschist along with volcanic rocks and gabbrodiorite masses infiltrating them (Figure 2). These rocks are affected by a phase of regional metamorphism of lower greenschist facies and at least two phases of deformation (Geravand, 2012). In the past, most researchers dated these rocks back to Precambrian epoch (Gansser, 1951; Stöcklin, 1968; Jenny, 1977*a*), but only recently, according to the findings of the Palynomorphs in the area, they have been dated back to Late Ordovician age (Ghavidel Sivaki et al., 2011).

3. Methodology

After collecting basic information of works done in the study area using aerial photographs and geological maps, all outcrops related to these rocks were identified and sampled in a field investigation in three steps for 13 days during the summer of 2015 and 2016. The optical analyses were performed by Olympus BX-41 polarizing microscope at the Department of Geology, Science and Research Branch, Islamic Azad University, Tehran, Iran. After detailed petrographic studies 17 fresh samples were analyzed using a Varian Liberty 200 inductively coupled plasma–atomic emission spectrometer (ICP-AES) for major elements and using a Perkin Elmer Optima 3300 DV inductively coupled plasma–optical

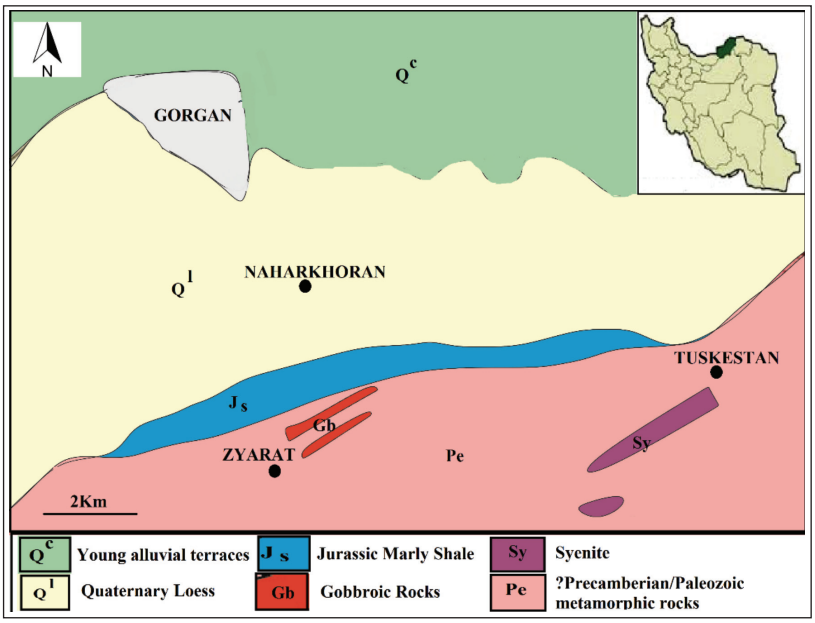

Figure 2- Location of the study area (adapted from the 1:250000 Scale map of Gorgan, Geological Survey of Iran).

emission spectrometer (ICP-OES) for trace and REE elements at Zamin Rizkavan lab, Iran. The data was interpreted using Minpet and GCDKIT 2.3 software.

4. Results

4.1. Field Study and Petrography

The mafic dykes are 1 to 5 meter in width and several hundred meters in length. They are surrounded by greenschists and show weak metamorphism (Figure 3). The samples have mesocratic to melanocratic color index (Figure 4). They have a gabbroic composition, with medium to large-grain size. They show ophitic to intergranular textures under polarized microscope (Figure 4).

The common mineralogical assemblage of gabbro and gabbrodiorite rocks in the region is plagioclase, pyroxene and opaque minerals. The plagioclases are generally subhedral to anhedral in shape (Figure 4) and sometimes they found as inclusions in pyroxene (Figure 4). Some of the clay minerals, might have formed by weathering of plagioclase prior to hydrothermal alteration. Apatite (Figure 4 e, f) and quartz are minor minerals in the rock. Gabbroic rocks of the region are heavily affected by deformation and metamorphism and show a wide range of secondary minerals such as epidote, chlorite, calcite and sericite (Figure 4 e, f). Intergranular, subophitic, and ophitic (Figure 4 a, b) and microgranoular textures are among the dominant textures in these rocks.

4.2. Geochemistry

The geochemical analysis of major, trace and rare earth elements of the study rocks are presented in table 1 and 2. FeOt is calculated by Le-Maitre's (1976) method.

Figure 3- Field photographs of samples in southern Gorgan.

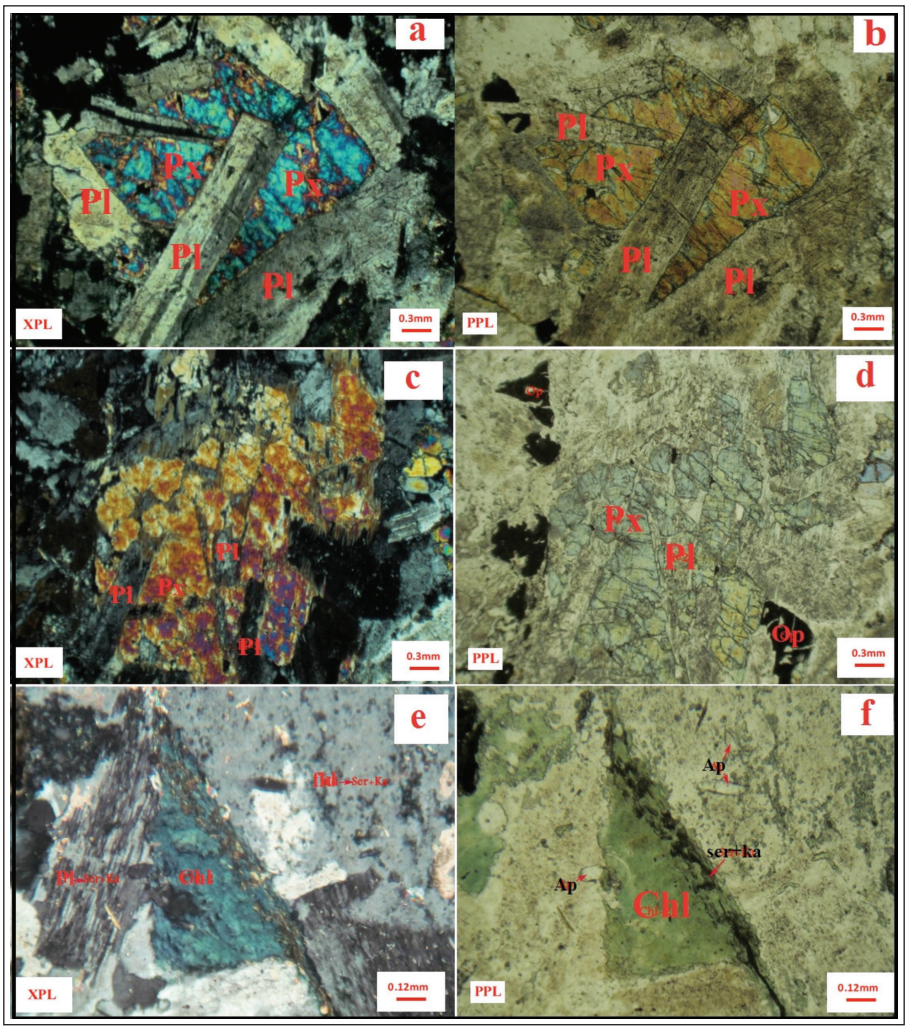

Figure 4- a, b) Ophitic textures in gabbros, c, d) Plagioclases as inclusion in pyroxene and opaque minerals, e. f) Sericite and plagioclase feldspars and along with secondary chlorite and abundant inclusions of apatite. Mineral Abbreviations (Kretz, 1983): Plagioclase: Pl, Pyroxene: Px, Chlorite: Chl, Apatite: Ap.

The classification diagram of SiO_2 (wt. %) vs. Na_2O/K_2O proposed by Winchester and Floyd (1977) is used for classification of intrusive rocks. According to this diagram, all samples are classified as gabbro (Figure 5).

Based on magma series diagrams (Irvine and Baragar, 1971), the samples are in (Figure 6a). But in the Nb/Y vs. (Zr/TiO_2* 0.0001) diagram (Winchester and Floyd, 1977) the samples are clearly in the alkaline range field (Figure 6b).

4.3. Origin

Chondrite normalized spider diagram of the samples is presented in figure 7a. The enrichment rate has been multiplied by 10-100 times. Plagioclase is the most prevalent and abundant mineral in the rocks of the study area. Sr and Ba enrichment is related to plagioclase. There is also negative anomaly in the elements Rb and K, indicating non-involvement of magma with continental crust (Kamber, 2012).

In the primitive mantle normalized diagram (Figure 7b), the studied samples show negative Rb anomaly. In the rocks affected by the deformation and metamorphism, this element is usually considered as mobile element (Kerrich and Manikyamba, 2011). Similarly, in the diagram normalized with chondrite and primitive mantle, there is no negative anomaly of high field strength elements such as Ti, P and Nb. This is a typical feature of intra-plate alkaline magmatic activity (Dai et al., 2011) and also suggests

Table 1- Results of major element analysis of the Zyarat gabbroic rocks.

Sample (wt.%)	A4	A5	B10-1	B12	B16-1	B16-2	B21-1	B21-2	B23-1	B23-2	B24-1	B24-2	B38	B39	B40	x	Bx-1
SiO_2	50.25	49.7	51.99	45.98	45.89	46.89	46.54	46.67	44.27	43.69	45.63	45.65	52.87	52.87	48.79	45.38	48.81
TiO_2	1.95	1.92	1.93	2.17	2	2	2.04	2.02	3.31	3.51	4.02	4	1.76	1.94	1.51	3.75	1.53
Al_2O_3	16.97	16.59	17.14	16.34	16.37	17.43	17.31	17.57	15.03	14.9	14.99	14.42	17.13	14.84	16.33	14.55	16.55
Fe_2O_3	3.78	4.54	3.92	3.45	3.67	3.74	3.2	3.17	4.62	4.48	4.68	4.55	3.8	4.17	3.76	4.75	3.67
FeO	5.31	5.03	4.31	5.99	5.86	5.74	5.13	5.07	7.7	7.83	7.47	7.28	5.59	5.97	6.27	7.6	5.64
MnO	0.14	0.13	0.11	0.14	0.13	0.13	0.13	0.13	0.14	0.15	0.16	0.19	0.22	0.19	0.16	0.18	0.14
MgO	5.95	6.8	2.91	5.8	6.01	5.85	4.76	4.59	5.78	5.77	4.42	4.93	2.47	3.88	5.98	4.3	6.47
CaO	6.24	7.05	4.34	9.14	9.22	9.67	10.14	9.81	8.85	8.79	9.27	9.69	7.25	4.77	8.82	7.86	8.77
Na_2O	5.06	4.44	6.51	3.61	3.37	3.27	4.03	4.13	3.15	3.01	3.27	3.52	5	6.09	3.73	4.24	3.93
K_2O	0.02	0.03	0.62	0.28	0.65	0.69	0.12	0.12	0.91	0.86	0.98	0.91	0.07	0.02	0.06	0.37	0.02
P_2O_5	0.19	0.17	0.62	0.43	0.48	0.52	0.32	0.32	0.37	0.4	0.41	0.48	0.5	0.51	0.19	1.23	0.17
BaO	<0.01	<0.01	0.07	0.04	0.08	0.08	0.02	0.02	0.09	0.08	0.07	0.08	0.02	<0.01	0.01	0.04	<0.01
Cr_2O_3	0.03	0.03	<0.01	0.02	0.02	0.02	0.03	0.03	0.01	0.01	<0.01	<0.01	<0.01	<0.01	0.03	<0.01	0.03
SrO	0.03	0.05	0.05	0.07	0.09	0.09	0.08	0.18	0.06	0.05	0.08	0.2	0.05	0.01	0.06	0.09	0.03
LOI	3.46	3.45	3.83	3.57	3.82	3.48	3.89	3.67	4.11	4.32	2.4	2.64	4.25	3.79	3.23	5.23	3.13
Total	99.38	99.93	98.35	97.03	97.66	99.6	97.74	97.5	98.4	97.85	97.85	98.54	100.98	99.05	98.93	99.57	98.89

Table 2- Results of trace element analysis of the Zyarat gabbroic rocks.

Sample	A4	A5	B10-1	B12	B16-1	B16-2	B21-1	B21-2	B23-1	B23-2	B24-1	B24-2	B38	B39	B40	B9-2	Bx-1
ppm																	
Ba	167.2	164	677.2	352.9	750	697.6	164.8	193.5	806.6	698.4	685.6	650.9	211.9	138.1	199.8	346	140.7
Co	42.1	39.2	18.6	40.1	41	39	35.6	31.5	51.3	48.6	43.2	44.5	16.2	29.2	44.1	36.7	39.3
Cr	196	205	11	165	138	128	229	221	83	87	<10	13	25	15	203	11	218
Cs	6.6	5.71	3.26	2.25	3.72	3.48	2.46	1.61	3.58	4.05	6.51	6.45	1.14	0.55	0.56	3.96	3.35
Ga	20.5	16.4	20.4	19.2	19.9	20.5	20.3	f20.7	21.4	20.4	23.3	22.6	29.7	29.5	19.2	22.3	19.5
Hf	2.6	2.3	6.5	4.1	4.3	3.9	4.3	4.4	4.1	4.3	5.5	5.6	10	13.1	2.3	5.3	2.4
Nb	19.5	18.1	51.9	31.7	37.2	34.1	30.2	32.2	24.8	25.3	49	36.7	61.5	80	29.2	50.8	29.6
Ni	103.1	96.7	16.1	90.2	95.8	94	70.8	63	86.8	81.1	22	22.7	14.7	28.9	89.4	9.7	90.9
Rb	0.3	0.8	10.8	5.5	16.4	16.3	2.7	2.5	26.1	23.9	39.1	34.8	1.2	<0.2	1.2	11.4	<0.1
Sc	17.5	20.7	11.3	24.9	20.4	18.9	31.7	27.2	49.1	46.1	33.6	36.1	19.8	23.3	26.5	22.3	22.8
Sn	<5	<5	<5	<5	<5	<5	<5	<5	<5	<5	<5	<5	<5	6	<5	<5	<5
Sr	283.5	461.4	505.1	702.6	970.1	919.9	897.8	926	577.5	567.3	846	930.9	552.7	449.3	592.6	949.1	325.6
Ta	1.7	1.6	3.7	2.2	2.3	2.1	2.2	2.4	1.8	1.9	3	2.8	4.3	5.6	1.7	3.7	1.7
TC	0.07	0.09	0.42	0.08	0.2	0.07	0.27	0.2	0.3	0.32	0.02	0.04	0.56	0.52	0.04	0.61	0.04
Th	2.64	2.01	5.16	2.78	2.75	2.6	2.48	2.78	2	1.92	3.88	3.79	7.27	5.32	1.94	4.51	1.75
TS	0.01	0.01	0.01	0.13	0.05	0.06	0.01	0.06	<0.01	<0.01	0.07	0.09	<0.01	<0.01	0.02	0.04	0.04

Table 2- continued.

Sample	A4	A5	B10-1	B12	B16-1	B16-2	B21-1	B21-2	B23-1	B23-2	B24-1	B24-2	B38	B39	B40	B9-2	Bx-1
ppm																	
U	0.32	0.29	1.04	0.78	0.93	0.82	0.87	0.78	0.63	0.64	1.03	1.05	1.98	2.61	0.27	1.24	0.61
V	159	192	99	193	180	169	205	194	483	487	392	389	79	107	248	265	210
W	1	<1	2	1	1	1	<1	<1	1	<1	1	1	2	2	<1	1	<1
Y	28	16.6	41.3	23.9	25.6	24.9	22.6	23.2	24.9	25.7	30.2	32.8	56.3	68.9	18.5	42.5	19.1
Zr	197	179	264	166	169	157	167	172	147	147	198	210	395	316	187	230	191
La	19.7	20.2	56.8	25.6	29.5	28.5	26.5	25.4	23.5	22.3	31.1	34	67.6	79.5	19.7	46.5	20.6
Ce	52.9	51.1	112.9	52.9	60.9	58.9	48.7	51.2	48.7	49	64.3	71.4	142.4	167.8	41.7	98.1	42.2
Pr	7.02	6.84	13.28	6.41	7.4	7.12	5.89	6.09	6.12	6.21	7.76	8.66	17.28	20.33	8.07	12.08	6.12
Nd	23.2	22.8	52.7	26.1	29.6	29	23.8	24.4	25.7	26.4	31.9	35.6	68.2	79.3	23.2	49.9	23.8
Sm	3.22	3.05	10.41	5.47	6.07	5.85	4.95	5.28	5.83	5.85	6.86	7.67	13.41	15.6	3.3	10.43	3.29
Eu	1.17	1.21	3.83	1.98	2.19	2.13	1.83	1.9	2.08	2.06	2.43	2.5	4.78	4.87	1.34	3.19	1.31
Gd	3.53	3.55	10.46	5.59	6.47	5.99	5.22	5.45	5.88	6.34	6.96	7.86	13.41	15.49	3.81	10.75	3.69
Tb	0.6	0.57	1.59	0.86	0.99	0.94	0.83	0.86	0.92	0.97	1.12	1.28	2.1	2.43	0.62	1.59	0.65
Dy	3.36	3.3	8.03	4.43	5.06	4.72	4.47	4.47	4.96	5.19	5.82	6.44	10.98	13	3.41	8.06	3.53
Ho	0.63	0.59	1.55	0.85	0.93	0.88	0.85	0.85	0.9	0.95	1.11	1.19	2.03	2.52	0.66	1.54	0.69
Er	1.75	1.68	4.19	2.29	2.43	2.36	2.32	2.35	2.43	2.47	2.96	3.16	5.6	6.86	1.81	4.05	1.76
Tm	0.23	0.22	0.54	0.31	0.33	0.31	0.29	0.31	0.31	0.32	0.4	0.42	0.74	0.93	0.24	0.51	0.24
Yb	1.49	1.33	3.2	1.94	1.92	1.84	1.84	2.01	1.9	1.93	2.46	2.58	4.59	5.75	1.48	3.2	1.57
Lu	0.21	0.21	0.51	0.27	0.3	0.27	0.27	0.29	0.27	0.26	0.36	0.38	0.7	0.87	0.23	0.47	0.23
Ce/Yb	35.5	38.42	35.28	27.27	31.72	32.11	26.47	25.47	25.63	25.39	26.14	27.67	31.04	29.18	28.17	30.66	26.88
Lu/Yb	0.14	0.16	0.16	0.14	0.16	0.15	0.17	0.14	0.14	0.13	0.15	0.15	0.15	0.15	0.15	0.15	0.15
La/Yb	13.22	15.18	17.75	13.19	15.36	15.49	14.40	12.63	12.36	11.73	12.64	13.17	14.72	13.82	13.31	14.53	13.12
Nb/U	60.9	62.41	49.9	40.64	40	41.5	44.71	41.28	40.65	49.5	47.61	33.01	41.55	108.1	37.3	42.3	48.52

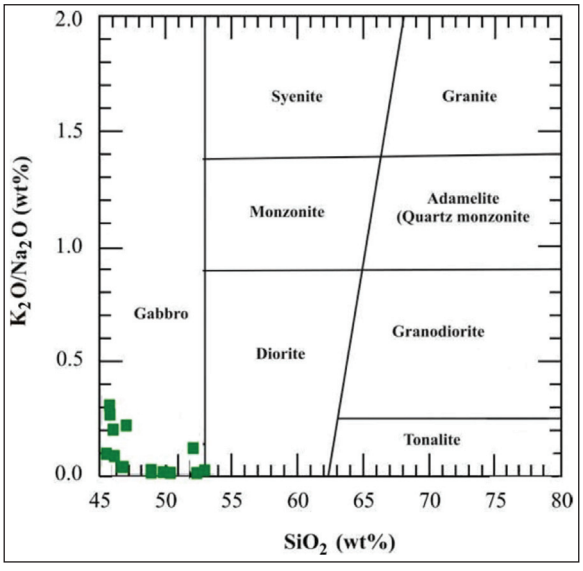

Figure 5- Rock classification diagram of the studied samples (Winchester and Floyd, 1977).

that there is no contamination of magma by continental crust (Ali et al., 2011). Slight Th in gabbros is probably due to combination of source rocks in the depth or at small melting dedree.

The samples are also normalized to OIB (Figure 7c). There is only a negative anomaly in the elements Rb and K, but the trend in the rest of the elements is consistent with the elements in the OIB.

High levels of Zr and Y in the studied samples suggest that primitive magma of gabbro is alkaline, because Zr is an incompatible element which goes into liquid phase immediately in the event of melting. The high ratio of La/Ta and Zr/Nb indicate high- alkaline magma erupting in intra-plate setting (Curtis et al., 1999).

The samples were normalized to chondrite in figure 8a and primitive mantle in figure 8b. In these diagrams, the samples show 10-100 times as much enrichment to chondrite and primitive mantle. A negative slope can be seen. In fact, the main feature of these samples is enrichment of LREE (Light Rare Earth Elements)

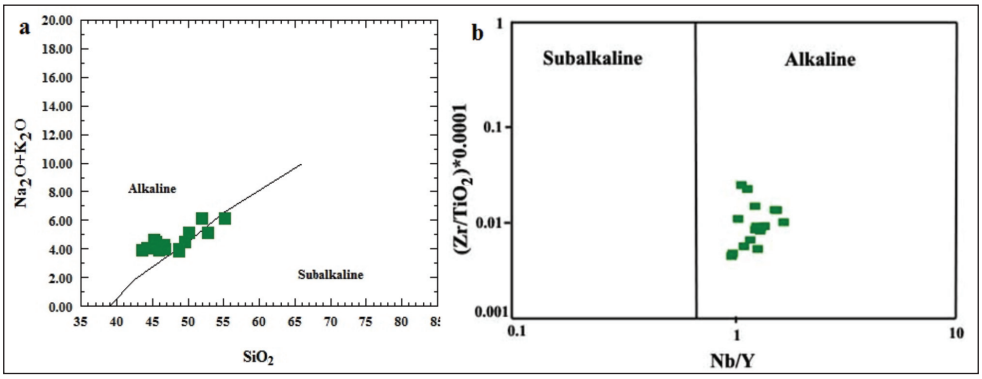

Figure 6- a) Total Alkali-SiO_2 (TAS) (Irvine and Baragar, 1971), and b) Nb vs (Zr/TiO_2) * 0.0001) (Winchester and Floyd, 1977) diagrams of the studied rocks.

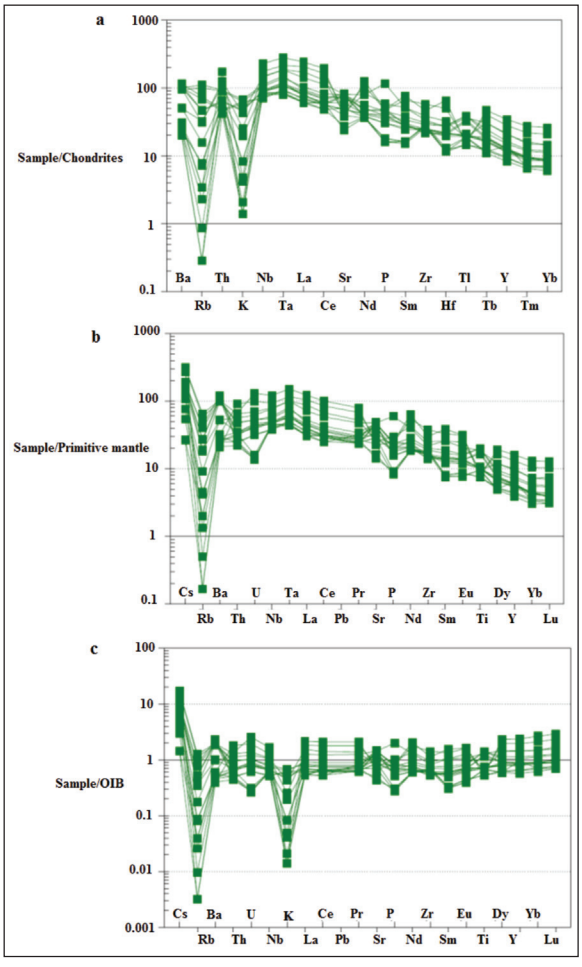

Figure 7- a) Chondrite-normalized spider diagram (Thompson, 1982), b) Primitive mantle-normalized spider diagram (Sun and McDonough, 1989), c) OIB-normalized spider diagram (Sun and McDonough, 1989) for the studied samples.

compared to HREE (High Rare Earth Elements). This indicates that the parent magma of rock including garnet and pyroxene have not participated in the melting and have retained heavy rare earth elements in refractory mantle (Rollinson, 1993; Zhao and Zhou, 2007). The LREE enrichment relative to HREE indicates a low-degree partial melting and high values of these elements in the source rock (Wright and McCurry, 1997). Similarly, it indicates the alkaline magma generated in intra-plate settings in interlayer space (Ali and Ntaflos, 2011). There is no Eu anomaly in REE plot.

According to the trend of samples on the REE diagram (Figure 8), it can be concluded that LREE are more compatible than HREE in parental gabbro magma. Depletion in heavy elements is attributed to presence of garnet in the source. LREE show enrichment to chondrites and primitive mantle. This suggests that magma derived from partial melting of mantle (Rollinson, 1993).

The samples were also normalized to OIB (Figure 8c). There is enrichment up to 2 times. The REE patterns of the studied rocks are very similar to OIB, and exhibit almost parallel trend to the OIB reference line passing through "1" (Figure 8).

5. Discussion

La/Yb ratios are high (10–21.4) in all samples (Table 2). The low La/Yb ratios reflect a melting regime dominated by relatively large melt fractions and/or spinel as the predominant residual phase (e.g., Falloon et al., 1988; Riley et al., 2005; Yang et al., 2007*a*) whereas high La/Yb ratios are indicative of smaller melt fractions and/or garnet control. The Nb/U ratios in Zyarat rocks are 40-60. These values are similar to those of the OIB (Nb/U= 47+10, Hofmann,

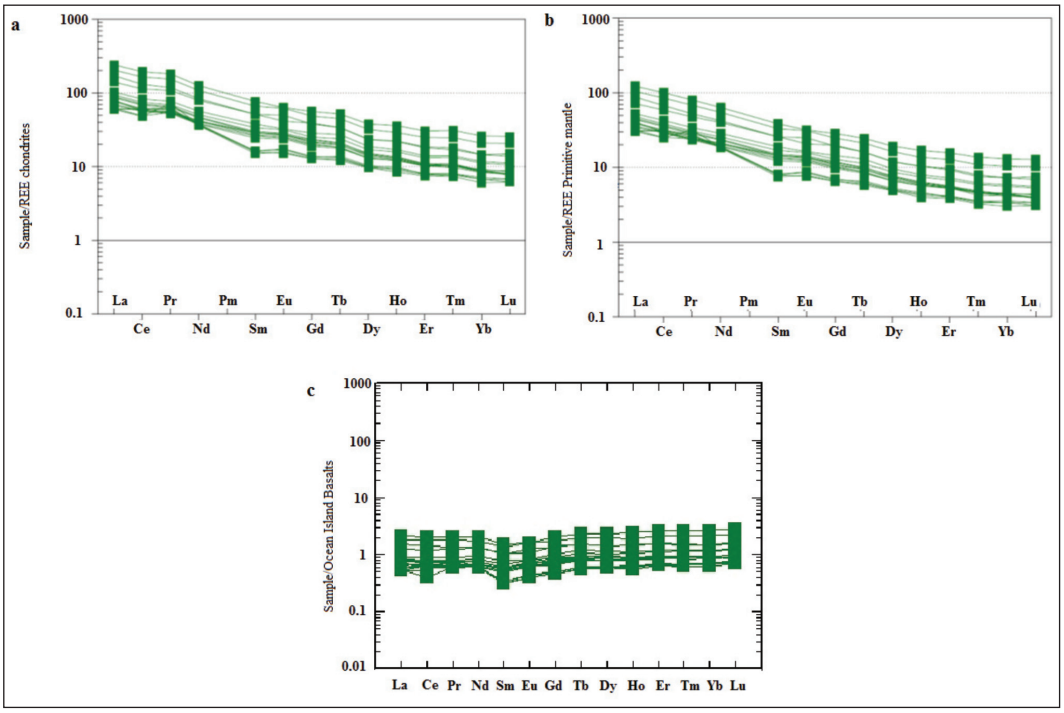

Figure 8- a) Chondrite-normalized REE diagram (Nakamura, 1974), b) Primitive mantle-normalized REE patterns (Sun and McDonough, 1989), c) OIB-normalized REE chart (Sun and McDonough, 1989) for the studied samples.

1988). The high LREE/HREE ratios and low Y content corresponding high Ti/Y ratios of the gabbros suggest that they could be derived from small melt fractions of a garnet stable source. Zr and Y do not fractionate significantly during partial melting (e.g., Yang et al., 2007*a*).

However, the dykes display low Rb/Sr (<0.1) and high Ba/Rb (>10). All of the dykes are enriched in LILE and LREE and depleted in Nb and Ta anomalies which are suggesting that metasomatism of source were triggered by subduction–related fluids or melts. Thus, the geochemical data indicate that all of the dykes may have formed by relatively low–percentage melting of an amphibole–bearing (Dai et al., 2011), refractory lithospheric mantle source in the garnet stability field. It may be metasomatized by recycled crustal materials prior to generation.

Pearce (2008) considers the melting of a low-depleted mantle to form a MORB and melt a relatively rich source (probably a mantle column at a greater depth) to form the OIB. There is a great similarity between the characteristics of the incompatible elements and the REEs of the alkaline samples and the OIB, which indicates the origin of taking the magma forming the rocks of the region from a mantle similar to the source of the OIB. In a diagram of Nb / Yb versus Th / Yb (Pearce, 2008), the samples are in the OIB range (Figure 9).

In a diagram of Nb against Nb/U (Cornelius et al., 2011), the ratio of Nb/U of studied rocks is high (Figure 10). Based on this diagram, the studied samples are in the range of OIB and away from the continental crust, which indicates the absence of crustal contamination

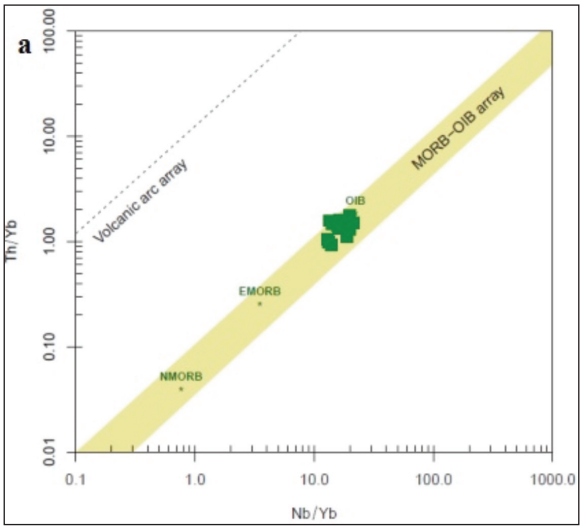

Figure 9- Nb/Yb vs Th/Yb diagram of the studied samples (Pearce, 2008).

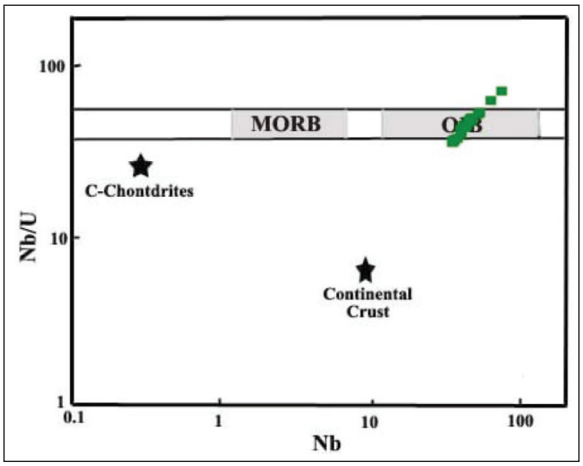

Figure 10- The Nb vs Nb/U diagram of studied samples (Cornelius et al., 2011).

in the evolution of gabbroic rocks. Dai et al. (2011) believe that magma derived from the mantle has low Lu/Yb ratio with average of 0.14-0.15, while this ratio is higher in the continental crust with average of about 0.16-0.18. The average Lu/Yb ratio in gGabbroic rocks is 0.15 which is less than that of the continental crust, and derivation of magma from these rocks from a mantle source shows no crustal contamination with the continental crust.

In order to detect the enrichment of origin of gabbroic rocks of Naharkhoran Valley, Zr-Y diagram was used (Sun and McDonough, 1989). These elements have very little mobility and are also used to study old igneous territories in high degrees of alteration (Prytulak and Elliott, 2007). All of the samples in the above-mentioned diagram are plotted in the field of enriched mantle (Figure 11a). Also in the Zr-against-Nb diagram (Abu-Hamatteh, 2005), the studied samples are in the field of enriched mantle (Figure 11b).

High Nb/Th ratio is one of the characteristics of oceanic crust (Rudnick and Fountain, 1995). This ratio is high in studied gabbros. In Nb/Th against Th diagram, the samples are in the range between enriched mantle and OIB (Figure 12a). The Rb/La against Th diagram also confirms it (Figure 12b). Both these diagrams show a lack of involvement of continental crust.

Based on geochemical analysis, the study rocks are in gabbro and the magma making these rocks had been

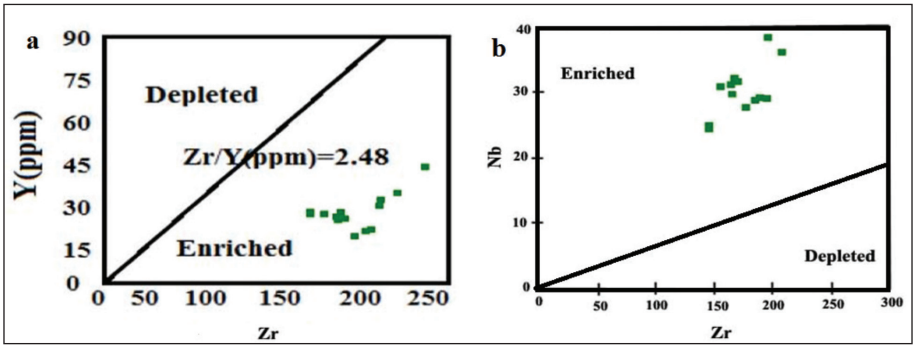

Figure 11- a) Y vs Zr (Sun and McDonough, 1989), and b) Zr vs Nb diagrams (Abu-Hamatteh, 2005) of studied rocks.

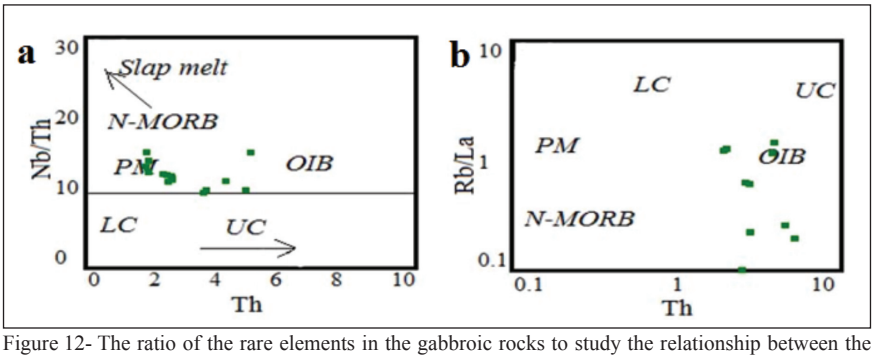

Figure 12- The ratio of the rare elements in the gabbroic rocks to study the relationship between the rocks with the enriched mantle, the upper crust and the oceanic islands (Zhao and Zhou, 2007); a) Nb / Th vs Th, and b) Rb / La vs Th diagrams of the studied samples.

alkaline in nature. Geochemical studies revealed that the gabbros were rich in K_2O and poor in Na_2O, and are mostly of alkaline type. According to Coleman and Donato (1979), high Na_2O and K_2O in gabbros resulted from exchanges with sea water or delayed magmatic vapor phase, which carries K_2O away and destroys it (Sinton and Byerly, 1980). The studied gabbros belong to alkaline magma series. The ratio of K_2O/P_2O_5 is used as an indicator for crustal contamination of magmas. Most of magmas originating from the mantle have a ratio of $K_2O/P_2O_5 < 2$. This ratio is 0.89 in average for the gabbros of the study area, indicating their origination from the mantle and absence of crustal contamination in them. The Nb value indicates the intraplate origin of these rocks. Gabbroic magma does not show depletion of Ti, Ta and Nb, suggesting non-participation of crustal materials or fluids derived from the crust in forming magma. Negative and steep slope of REE plot in these rocks suggests deep origination and reveals an origin associated with enriched mantle. High Fugacity of CO_2/H_2O in magma origin as well as a small degree of partial melting is among possible reasons for such a trend. Moreover, HREE depletion indicates that garnet and zircon have remained in the melting residue. The REE plot of the gabbros is similar to OIB, suggesting that both gabbros and OIB magmas share the same origin.

6. Conclusion

A suite of mafic gabbro dykes are intruded in the Middle–Upper Paleozoic rock units representing a part of the north Gondwana province. The alkaline gabbros include plagioclase, clinopyroxen and small needle of apatite. In general, they show OIB-like trace element patterns characterized by enrichment in LILE and LREE. Negative anomalies of Rb and K and Pb positive anomalies of Nb and Ti in the spider diagrams and other geochemical variations observed in studied rocks all indicate uncontamination by crust. Accordingly, the samples are located within the OIB range away from the continental crust, which indicates the absence of crustal deformation in the gabbroic rocks of the study. The high La / Yb ratio in the studied samples can reflect small degree of melting or garnet presence in the mantle. The tectonic environment of mafic dyke can be assigned to the initiation of the opening of Paleotethys in northern part of Gondwana province in late Ordovician time.

Acknowledgements

We would like to thank Dr. Reza Fahim Guilany for contributing the development of this article with his critiques.

References

Abu-Hamatteh, Z.S.H. 2005. Geochemistry and petrogenesis of ma.c magmatic rocks of the Jharol Belt, India: geodynamic implication. Journal of Asian Earth Sciences 25, 557-581.

Alavi, M. 1991. Sedimentary and structural characteristics of the Paleo–Tethys remnants in northeastern Iran. Geological Society of America Bulletin 103, 983-992. Doi: 10.1130/0016-7606(1991)103<0983:SASCOT>2.3.CO;2

Alavi, M. 1996. Tectonostratigraphic synthesis and structural style of the Alborz mountain system in northern Iran. Journal of Geodynamics 21, 1-33.

Ali, K.A., Moghazi, A.M., Moufti, M.R. 2011. Geochemistry and Sr-Nd-Pb isotopic composition of the Harrat Al-Madinah Volcanic Field, Saudi Arabia. Gondwana Research 21(2-3), 670-689. doi:10.1016/j.gr.2011.06.003

Ali, S., Ntaflos, T. 2011. Alkali basalts from Burgenland, Austria: Petrological constraints on the origin of the westernmost magmatism in the Carpathian-Pannonian Region. Lithos 121(1-4), 176-188.

Allen, M.B., Ghassemi, M.R., Shahrabi, M., Qorashi, M. 2003. Accommodation of late Cenozoic oblique shortening in the Alborz range, northern Iran. Journal of Structural Geology 25, 659-672. Doi: 10.1016/S0191-8141(02)00064-0

Berberian, M., King, G.C. 1981. Towards a palegeography and tectonic evolution of Iran. Cannadian Journal of Earth Sciences 18, 210-265. https://**doi**.org/10.1139/e81-019.

Brunet, M.F., Ershov, A.V., Korotaev, M.V., Nikishin, A.M. 2003. The South Caspian basin: a review of its evolution from subsidence modelling. Sedimentary Geology 156, 119-148. Doi: 10.1016/S0037-0738(02)00285-3.

Coleman, R.G., Donato, M.M. 1979. Oceanic plagiogranite revisited. Barker, F. (Ed.). Trondhjemites, Dacites and Related Rocks. Elsevier, Amsterdam, 149-168.

Cornelius, T., NtaAos, Th.V., Akinin, V. 2011. Polybaric petrogenesis of Neogene alkaline magmas in an extensional tectonic environment: Viliga Volcanic Field, northeast Russia. Lithos 122, 13-24.

Curtis, M.P., T., Leat, B., Millar, Randall, Riley, I., Storey, D. 1999. Middle Cambrian rift-related volcanism in the Ellsworth Mountains, Antarctica: tectonic implications for the paleo-Pacific margin of Gondwana. Tectonophysics 304, 275-299.

Dai, J., Wang, C., Hébert, R., Li, Y., Zhong, H., Guillaume, R., Bezard, R., Wei, Y. 2011. Late Devonian OIB alkaline gabbro in the Yarlung Zangbo Suture Zone: Remnants of the Paleo–Tethys? Gondwana Research 19, 232-243.

Davoudzadeh, M., Lensch, G., Weber–Diefenbach, K. 1986. Contribution to the paleogeography, stratigraphy and tectonics of the Infracambrian and Lower Paleozoic of Iran. Neues Jahrbuch fur Geologie und Palaontologie Abhandlungen 172, 245-269.

Davoudzadeh, M., Weber–Diefenbach, K. 1987. Contribution to the paleogeography, stratigraphy and tectonics of the Upper Paleozoic of Iran. Neues Jahrbuch fur Geologie und Palaontologie Abhandlungen 175, 121-146.

Delaloye, M., Jenny, J., Stampli, G. 1981. K–Ar dating in the eastern Elburz (Iran). Tectonophysics 79, 27-36.

Falloon, T.J., Green, D.H., Hatton, C.J., Harris, K.L. 1988. Anhydrous partial melting of a fertile and depleted peridotite from 2 to 30 kbar and application to basalt petrogenesis. Journal of Petrology 29, 1257-1282. doi:10.1093/petrology/29.6.1257

Gansser, A. 1951. Geological reconnaissance in Gorgan and surrounding area. National Iran Oil Company, interal geological report no 10, 37 (unpublished).

Geravand, M. 2012. Natural pollution assessment of heavy metals in soils of Gorgan's schist. Master's thesis, Shahrood University of Technology, 156 p. Shahrood (unpublished).

Ghavidel Sivaki, M., Hassanzadeh, H., Vecoli, M. 2011. Palynology and isotope geochronology of the upper Ordovician–Silurian successions (Ghelli and Soltan Maidan Formation) in the Khoshyeilagh area, eastern Alborz Range, northern Iran; stratigraphic and palaeogeographic implications. Rewiew of Plalaeobotany and Palynology 164, 251-271.

Gorring, M.L., Kay, S.M. 2001. Mantle sources and processes of Neogene slab window magmas from southern Patagonia, Argentina. Journal of Petrology 42, 1067-1094. doi:10.1093/petrology/42.6.1067.

Hofmann, A.W. 1988. Chemical differentiation of the Earth: the relationship between mantle, continental crust, and oceanic crust. Earth and Planetary Science Letters 90, 297-314. doi: 10.1016/0012-821X(88)90132-X.

Horton, B.K., Hassanzadeh, J., Stockli, D.F., Axen, G.J., Gillis, R.J., Guest, B., Amini, A.H., Fakhari, M., Zamanzadeh S.M., Grove, M. 2008. Detrital zircon provenance of Neoproterozoic to Cenozoic deposits in Iran: Implications for chronostratigraphy and collisional tectonics. Tectonophysics 451, 97-122. Doi: 10.1016/j.tecto.2007.11.063

Irvine, T.N., Baragar, W.R.A. 1971. A guide to the chemical classification of the common volcanic rocks. Tectonophysics 451, 97–122.

Jenny, J.G. 1977*a*. Geologie et stratigraphie de l'Elbourz oriental entre Aliabad et Shahrud, Iran. These presentee la Faculte des Sciences de l'Universite de Genve, 1-238.

Jenny, J.G. 1977*b*. Precambrien et Paleozoique inferieur de l'Elbourz oriental entre Aliabad et Shahrud, Iran du nord–est. Eclogae Geologicae Helvetiae 70, 761-770.

Kamber, E. 2012. Back arc basing in the Coatmalia zone in Africa. Journal of Geophysical 92, 34-62.

Kerrich, R., Manikyamba, C. 2011. Geochemistry of alkaline basalts and associated high-Mg basalts from the 2.7 Ga Dharwar craton, Penakacherla Terrane. India: An Archean depleted mantle-OIB array. Precambrian Research 188, 104-122.

Kretz, R. 1983. Symbols for rock-forming minerals. American Mineralogist 68, 1-2, 277-279.

Le-Maitre, R.W. 1976. The chemical variability of some common igneous rocks. Journal of Petrology 17, 589-637.

Nakamura, N. 1974. Determination of REE, Ba, Fe, Mg, Na and K in carbonaceous and ordinary chondrites. Geochimica et Cosmochimica Acta 38, 757-775.

Pearce, J.A. 2008. Geochemical fingerprinting of oceanic basalts with applications to ophiolite classification and the search for Archean oceanic crust. Lithos 100, 14-48.

Prytulak, J., Elliott, T. 2007. TiO_2 enrichment in ocean island basalts. Earth and Planetary Science Letters 263, 388-403. Doi: 10.1016/j.lithos.2007.06.016

Raghimi, M. 2010. Tectono–magmatic setting of deformed plutonic rocks of Gorgan Schists in Naharkhoran, Gorgan–Iran. Gorgan University of Agricultural sciences and Natural Resources. Technical report. 56 p (unpublished).

Rahimi Chakdel, A. 2007. Geochemistry and petrogenesis investigations of igneous veins in Ziarat village of Gorgan, Gorgan University of Agricultural sciences and Natural Resources. Technical report. 47 p (unpublished).

Riley, T.R., Leat, P.T., Curtis, M.L., Millar, I.L., Dunca, R.A., Fazel, A. 2005. Early–Middle Jurassic dolerite dykes from western Dronning maud land (Antarctia): Identifying mantle sources in the Karoo large igneous province. Journal of Petrology 46, 1489-1524. http://dx.doi.org/10.1093/petrology/ego023

Rollinson, H.R., 1993. Using geochemical data, Evaluation, Presentation, Interpretation Addison: Wesley Longman, Harlow, 352 p.

Rudnick, R.L., Fountain, D.M. 1995. Nature and composition of the continental crust: a lower crustal perspective. Reviews of Geophysics 33, 267-309.

Salehi Rad, M.R. 1979. Etude géologique de la region de Gorgan (Alborz oriental, Iran) These de docteur 3em cycle.

Şengör, A.M.C. 1990. A new model for the late Palaeozoic–Mesozoic tectonic evolution of Iran and implications for Oman. Robertson, A.H.F., Searle, M.P., Ries, A.C. (Ed.), The Geology and Tectonics of the Oman region. Geological Society, London, 797-831.

Sharabi, M. 1990. Geological map of Gorgan 1:250000, Geological survey of Iran, Tehran.

Sinha A.K. 2012. Petrological characterization of Proterozoic mafic dykes from the Singhbhum craton, eastern India, 34th International Geological Congress, Brisbane, Australia.

Sinha, A.K. 2013. Geochemistry of distinct mafic dykes from the damodar valley gondwana basins and chhotanagpur gneissic terrain, eastern India: implications for their petrogenesis and tectonic setting, Geological Society of America Abstracts with Programs.

Sinton, J.M., Byerly, G.R. 1980. Silicic differentiates of abyssal oceanic magmas: evidence for late-magmatic vapor transport of potassium. Earth and Planetary Science Letters 47, 423-30.

Stampfli, G.M., Borel, G.D. 2002. A plate tectonic model for the Paleozoic and Mesozoic constrained by dynamic plate boundaries and restored synthetic oceanic isochrones. Earth and Planetary sciences letters 196, 17-33. http://dx.doi.org/10.1016/S0012-821X(01)00588-X

Stöcklin, J. 1968. Structural history and tectonics of Iran: A review. The American Association of Petroleum Geologists Bulletin 52, 1229-1258.

Stöcklin, J. 1974. Possible ancient continental margins in Iran. Burk, C.A., Drake, C.L. (Ed.). The geology of continental margins. Springer–Verlag; Berlin, Heidelberg, New York, 873–887.

Sun, S.S., McDonough, W.F. 1989. Chemical and isotopic systematics of oceanic basalts: implication for mantle composition and processes. Saunders, A.D., Norry, M.J. (Ed.). Magmatism in the Ocean Basins. Geological society, London, Speacial publications, 42, 313-345. doi:10.1144/GSL.SP.1989.042.01.19

Thompson, R.N. 1982. Magmatism of the British tertiary volcanic province. Scotland Geological Journal 18, 49-107.

Wendt, J., Kaufmann, B., Belka, Z., Farsan, N., Karimi Bavandpur, A. 2005. Devonian /lower and palaeogeography of Iran, Part II. Northern and central Iran. Acta geologica polonica 55, 31-97.

Winchester, J.A. Floyd, P.A. 1977. Geochemical discrimination of different magma series and their differentiation products using immobile elements. Chemical Geology 20, 325-343. http://dx.doi.org/10.1016/0009-2541(77)90057-2

Wright, J.B., McCurry, P. 1997. Geochemistry of calc-alkaline volcanic in northwestern Nigeria, and a possible Pan-African suture zone. Can, Earth and Planetary Science Letters 37, 90-96.

Yang, J.H, Wu, F.Y, Wilde, S.A, Xie, L.W, Yang, Y.H, Liu, X.M. 2007. Trace magma mixing in granite genesis: in–situ U–Pb dating and Hf–isotope analysis of zircons. Contributions to Mineralogy and Petrology 153, 177-190.

Yang, J.H., Sun, J.F., Chen, F., Wilde, S.A., Wu, F.Y. 2007. Sources and Petrogenesis of Late Triassic Dolerite Dikes in the Liaodong Peninsula: Implications for Post–collisional Lithosphere Thinning of the Eastern North China Craton. Journal of Petrology 48, 1973-1997.

Zamani Pedram, M., Hossieni, H. 2003. Geological map of Gorgan 1:100000, No. 6862, Geological survey of Iran, Tehran.

Zhao, J.H., Zhou, M.F. 2007. Geochemistry of Neoproterozoic mafic intrusions in the Panzhihua district (Sichuan province, SW China). Implications for subduction-related metasomatism in the upper mantle. Precambrian Research 152, 27-47. Doi: 10.1130/0016-7606(1991)103<0983:SASCOT>2.3.CO;2